Proceedings of Ninth World Conference on Earthquake Engineering
August 2-9, 1988, Tokyo-Kyoto, JAPAN (Vol.VI)

10-3-1

DYNAMIC BEHAVIOUR OF SHIELD TUNNEL DURING EARTHQUAKE

Naoto OHBO, Fumio NAGAI and Kazuo HAYASHI

Kajima Institute of Construction Technology, Chofu City, Tokyo, Japan

SUMMARY

In order to clarify three dimensional deformations of a shield tunnel due to earthquakes by using three seismometers installed in the tunnel, microtremor, artificial and natural earthquake observations in the tunnel were conducted. The shield tunnel with a circular cross section having a 9.5 m outer diameter is located in diluvial sandy soil beneath sea bed at a depth 22.5 m under sea level. It was found that the normal and vertical deformations to the tunnel axis changed with the epicentral distance and frequency components. These results show the necessity of the earthquake array observation consisting of more than two seismometers installed in a shield tunnel which is located in complex ground conditions and having different inter-connected structures.

INTRODUCTION

The earthquake resistant design of underground structures was made by the response displacement method in order to compute stresses and strains on the structure due to the deformations of the surrounding ground during earthquakes. The deformations of tunnels during earthquakes were described based on the results of earthquake observations of submerged tunnels, shield tunnels, and box section tunnels constructed in soft ground. However, the deformations of tunnels due to surrounding ground conditions and earthquake characteristics, such as seismic wave propagation of bed rock, epicentral distance, magnitude and frequency components, have not yet been sufficiently clarified.

Earthquake observations of shield tunnels are carried out by measuring the acceleration and the strain of tunnel elements in order to clarify a diformation of the shield tunnel (Refs. 1,2,3). However, three dimensional deformations of shield tunnels during earthquakes have not been well investigated. The purpose of this paper is to clarify the three dimensional deformations of a shield tunnel due to earthquake by using three seismometers actually installed in the tunnel.

OUTLINE OF OBSERVATION SITE

The observation site is located about 1 km north of Haneda Airport. Figure 1 shows the location of the shield tunnel. Figure 2 shows typical soil profiles and the location of the measuring instruments. The length of the large scale shield tunnel with a 9.5 m outer diameter is 3.3 km. The most portion of the tunnel lies beneath the Keihin Canal at a depth of 22.5 m below sea level (approximately 15 m

under the sea bed). Three seismometers were installed in position (points A, B and C, Fig. 1) in a straight line 90 m in length. Points A, B and C are located in diluvial sandy soil and about 1.2 km from the vertical shaft No. 2. The seismometers consisted of three components : axial, normal and vertical. Two were installed at the measurement points A and C, and third, using only axial and vertical directions, was installed at a measurement point B. The overall system is capable of simultaneously recording the 8 components of the particle velocity amplitude in the tunnel motion using servo-type accelerometers with integrators.

The dynamic behavior of the shield tunnel due to three different ground motions, such as microtremor, artificial and natural earthquakes, was observed. An artificial earthquake corresponds to the seismic waves generated from a large explosion. This explosion was set off at Yumenoshima which is located 7 km from the tunnel. In addition, a total of three natural earthquakes have been recorded since March 18, 1987. A schematic map of the locations of the recording station and the epicenter of the artificial and the three natural earthquakes is shown in Fig. 3. A list of the natural earthquakes and their characteristics is summarized in Table 1.

RESULTS

The deformation of the shield tunnel due to the three different ground motions is discussed by using displacement waveforms in which the motions were calculated from an integration of observed velocity waveforms.

Microtremor Microtremors have been widely recognized as a useful and convenient tool for obtaining information of the characteristics of the dynamic behavior of both ground and structures. In this case, an observation was made at midnight and a record was taken every 4 minutes. The microtremor records of the axial, normal and vertical displacement waveforms at the two measurement points A and C are shown in Fig. 4. The amplitude level of microtremor during the observation was about 0.3 microns. In Fig. 4, the close similarity of the records from two seismometers at the axial and normal directions is clearly seen. However, the vertical direction waveforms are slightly different.

Figure 5 shows the results of frequency analyses, such as Power Spectra and phase difference, of the axial, normal and vertical displacement waveforms observed at the two measurement points A and C. The amplitudes of the predominant frequencies for the axial and normal directions are the same. However, that of the vertical direction is remarkably different. The phase differences of the axial direction are distributed around 0 degree. It seems that the deformation of the axial direction to the tunnel axis due to the microtremor is uniform. However, those of the normal and vertical directions are distributed between -90 and 180 degree. These results indicate that the deformation of the normal and vertical direction is not uniform.

The predominant frequencies observed at the three measuring points are summarized in Table 2. The predominant frequency of each direction are the same. However, the amplitudes of the predominant frequency of the vertical direction at the two measurement points A and C are slightly different, and the phase differences are significantly greater.

Artificial Earthquake (Yumenoshima Explosion) A project to clarify the deep underground structure of the Metropolitan area of Tokyo by means of the seismic refraction method has been conducted since 1975. The location of the shot point for the Yumenoshima explosion is located around 7 km northwest of the shield tunnel (Fig. 3). 500 kg of dynamite was fired simultaneously at the bottom of a 100-110m deep bore hole. This explosion corresponds to a near field earthquake, although the wave generation energy is not as large as in a natural earthquake. In order to clarify the dynamic behavior of the shield tunnel due to the near field earthquake, artifi-

cial earthquake waveforms caused by this explosion were recorded by using an automatic starting measurement system. Figure 6 shows the recording of the artificial earthquake displacement waveforms of the axial, normal and vertical directions to the tunnel axis obtained at the measurement points A and C. The initial wave was identified as refracted P waves from the base rock (Refs. 4,5). The characteristics of waveforms between point A and C are slightly different.

Figure 7 shows the results of frequency analyses, such as Power Spectra and phase difference, of the axial, normal and vertical displacement waveforms observed at the two measurement points A and C. The frequency contents of the axial and normal directions at the two points are very similar. However, the predominant frequencies at the two measurement points for each direction are different. In particular, the characteristics of the vertical direction motions to the tunnel axis are remarkably different. The phase difference corresponds to the wave propagation velocity. The wave propagation velocity obtained from the phase difference of the predominant frequency at 4.49 Hz is 4.9 km/sec. This corresponds to the P wave propagation velocity of the base rock (Ref. 6).

The predominant frequencies of the artificial earthquake displacement waveforms at the three measuring points A, B and C are remarkably different (Table 2). However, those for each measurement point are almost the same. Figure 8 shows the three component waveform at the measurement points A and C, which were filtered through digital band pass filter with the central frequency of 4.49 Hz. The waveforms of the axial, normal and vertical directions are remarkably different. It can be considered that the response of the tunnel is affected by the traveling-wave effect and the surrounding ground conditions.

Natural Earthquake Figures 9 and 10 show the displacement waveforms recorded on the axial, normal and vertical direction to the tunnel axis due to Events No.1 and No.2 earthquakes. Event No.1, Fukusimaken-oki earthquake, had a distant epicenter, and Event No.2, Ibarakiken-Nanseibu earthquake, was caused by a deep fault in the near field (Table 1). They have a different incident angle to the tunnel axis (Fig. 3). In Figs. 9 and 10, the close similarity of the records between points A and C, apart from the vertical direction of Event No.2, are clearly seen. In Event No. 1, a long period component can be seen and the duration of the earthquake is long. However, Event No. 2 has several features of a near earthquake with deep fault, i.e. the short duration of main wave and a clear initial motion of the vertical direction.

Figures 11 and 12 show the Power Spectra and phase difference, which are obtained by the displacement waveforms of the three directions to the tunnel axis between points A and C. In Event No. 1, with the epicenter being at a greater distance from the shield tunnel, all three directions have a similar dominant frequency and the phase difference is small. However, in Event No. 2, with the epicenter being nearer the shield tunnel, the axial direction has a single dominant frequency, and the normal and vertical directions have several dominant frequencies. It is especially interesting that the frequency components between 2 and 3 Hz are similar to those in the artificial earthquake (Fig. 7). It appears that the deformations of the three directions for the long period predominant frequency are uniform. However, the deformations of the normal and vertical directions to the tunnel axis due to the near field earthquake are different form that of those due to the more distant earthquakes.

The predominant frequencies of the 8 components for Event No.1 and No.2 are also summarized in Table 2. The predominant frequencies of the three component waveforms at the points A, B and C due to Event No. 1, which has a distant epicenter, are closely related. Also, the predominant frequencies of the axial and vertical directions to the tunnel axis for Event No. 2, which is a near field earthquake, are almost the same. However, those of these two directions are different from the predominant frequency of the normal direction to the tunnel axis.

CONCLUSIONS

Through the observations of the dynamic behavior of the shield tunnel due to the three different ground motions, i.e. microtremor, artificial and natural earthquakes, the deformations of the axial, normal and vertical directions to the tunnel axis were investigated. The results can be summarized as follows :

1. The deformation characteristics of the shield tunnel show an influence by a traveling seismic wave.
2. The deformation of the axial direction to the tunnel axis of a long period ground motion is uniform.
3. The normal and vertical deformations to the tunnel axis are changed due to the epicentral distance and frequency spectrum.
4. The deformation of a shield tunnel due to the near field earthquake has to be clarified using an earthquake array observation.

Although these are conclusions drawn from the observed three different small tunnel motions, these results show the necessity of the earthquake array observation consisting of more than two seismometers installed in a shield tunnel to near field large earthquakes.

REFERENCES

1. Tamura C., Noguchi T. and Kato K., Earthquake Observation along Measuring Lines on the Surface of Alluvial Soft Ground, 6WCEE, 63-68, (1974).
2. Tamura C., Okamoto S., Kato K. and Kido Y., Deformation of Tunnel in Soft Ground During Earthquake, 8WCEE, 711- 718, (1984).
3. Suzuki T., Tamura C and Maeda H., Earthquake Observation and Response Analysis of Shield Tunnel, Proc. of the 7 Japan Earthq. Eng. Symp. 1903-1908, (1986).
4. Shima E., On the Base of Tokyo Metropolis, 7WCEE, 161-165, (1980).
5. Ohbo N., Hayashi K. and Nagai F., Dynamic Behavior of Shield Tunnel during Artificial Earthquake, Reprint of 18th Earthquake Engineering Research Meeting, JSCE, 497-500, (1987) (in japanese).
6. Seo K. and Kobayashi K., On the Rather Long-Period Earthquake Ground Motions Due to Deep Ground Structures of TOKYO Area, 7WCEE, 9-16, (1980).

Table 1 List of Earthquake

Event No.	Date	M	I*	Focal Depth (km)	Epicentral Distance (km)	Max ACC (gal)	Max Vel (kine)	Max Dis (cm)
1	1987.4.07	6.6	4	44	207	7.1	1.01	0.17
2	1987.4.10	4.9	3	60	45	11.3	0.65	0.05
3	1987.4.17	6.1	3	40	285	1.8	0.32	0.08

* : JMA Intensity at Tokyo

Table 2 Predominant Frequency of three different motions

Directions / Points	Axial A	Axial B	Axial C	Normal A	Normal C	Vertical A	Vertical B	Vertical C
Microtremor	0.78	0.78	0.78	0.83	0.83	0.81	0.81	0.81
Artificial	4.49	3.15	2.34	4.49	2.54	4.30	4.40	2.03
Event No.1	0.47	0.47	0.47	0.45	0.45	0.44	0.44	0.44
Event No.2	0.71	0.71	0.71	0.49	0.49	0.68	0.68	0.68

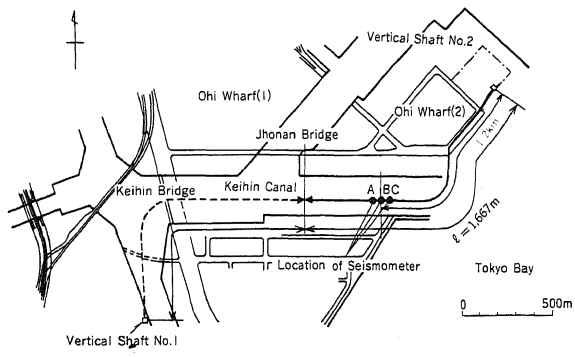

Fig. 1 Location of Shield Tunnel

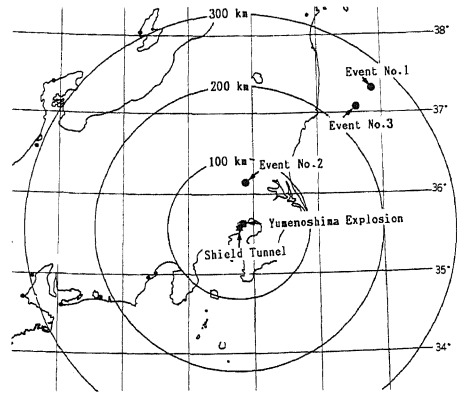

Fig. 3 Map of Location of Recording Point and Epicenter of Earthquakes

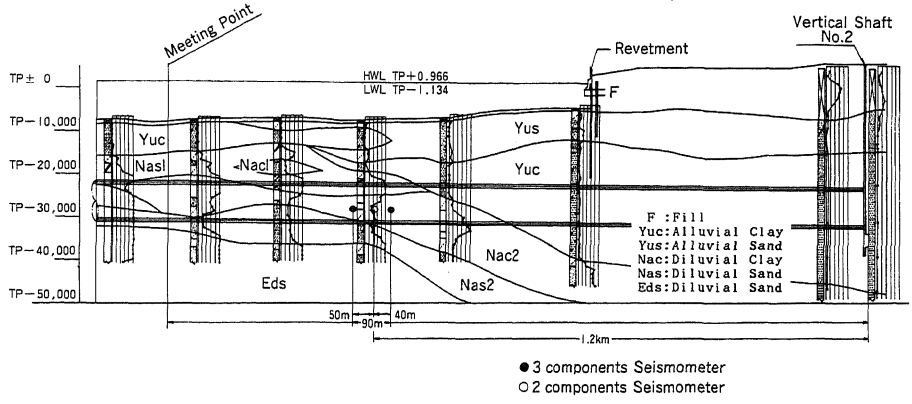

Fig. 2 Soil Profile and Location of Measurement Instrument

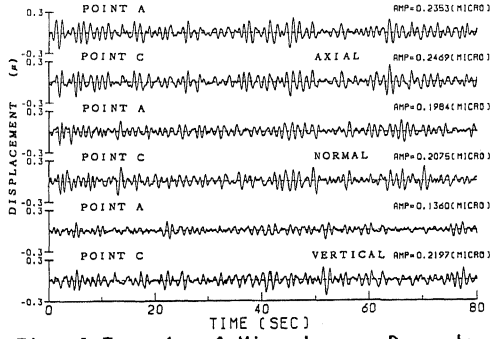

Fig. 4 Example of Microtremor Records

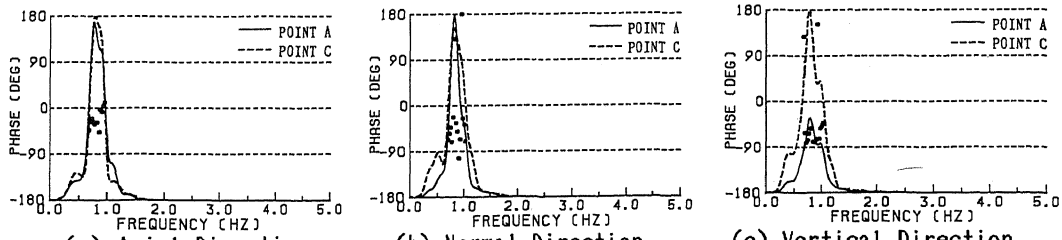

(a) Axial Direction (b) Normal Direction (c) Vertical Direction

Fig. 5 Power Spectra and Phase Difference for Displacement Waveforms

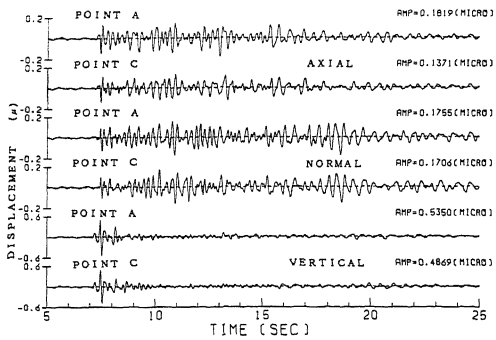

Fig. 6 Artificial Earthquake Waveforms

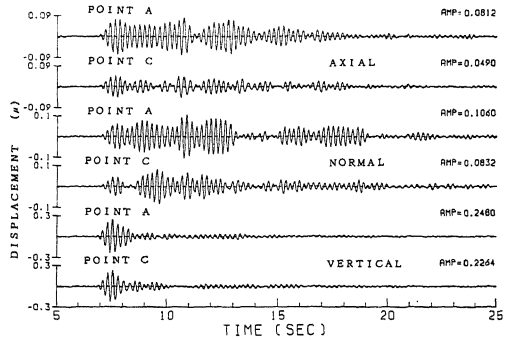

Fig. 8 Displacement Waveforms at 4.49 Hz

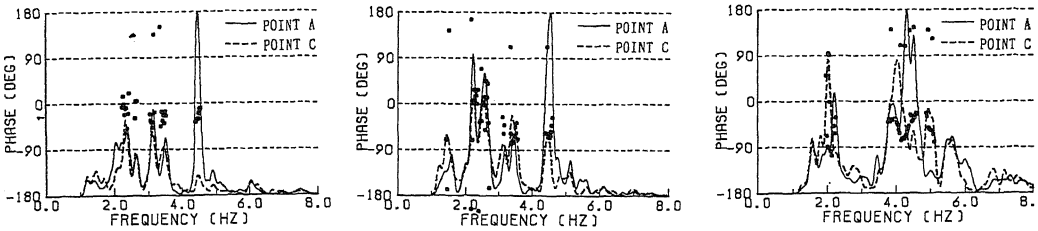

(a) Axial Direction (b) Normal Direction (c) Vertical Direction

Fig. 7 Power Spectra and Phase Difference for Displacement Waveforms

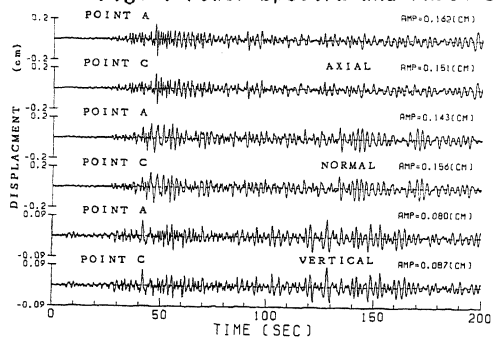

Fig. 9 Event No.1 Earthquake Waveforms

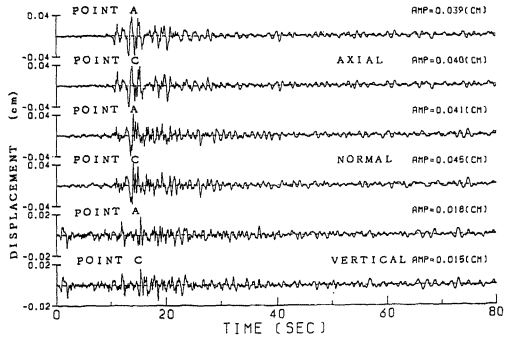

Fig. 10 Event No. 2 Earthquake Waveforms

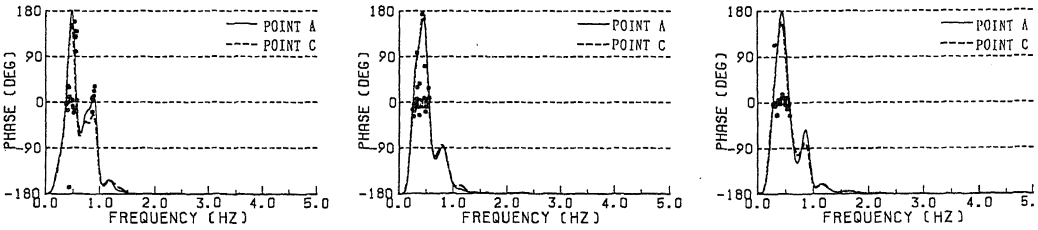

(a) Axial Direction (b) Normal Direction (c) Vertical direction

Fig. 11 Power Spectra and Phase Difference for Displacement component to Event No. 1

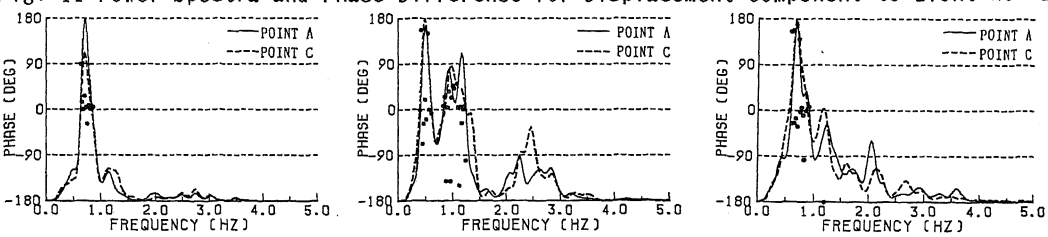

(a) Axial Direction (b) Normal Direction (c) Vertical Direction

Fig. 12 Power Spectra and Phase Difference for Displacement Component to Event No. 2